CrossMark

Particulate matter concentration levels during intense haze event in an urban environment

**Jamiu Adetayo Adeniran · Adeniyi Saheed Aremu ·
Yusuf Olatunji Saadu · Rafiu Olasunkanmi Yusuf**

Abstract This study assessed concentration levels of particulate matter (PM) in the ambient environment of Ilorin metropolis, Nigeria, during haze episodes. Meteorological data (wind speed and direction, rainfall data, sunshine data, relative humidity and temperature) were obtained. Aerocet 531S particle counter (MetOne Instruments, USA) was used to measure four mass concentration ranges of PM ($PM_{1.0}$, $PM_{2.5}$, PM_{10} and the total suspended particles (TSP)) in 10 locations taking into consideration land use patterns. Surfer® version 8 (Golden Software LLC, USA) was used to model the spatial variation of particulate matter concentration levels using kriging interpolation griding method. Human exposure assessment was done using the total respiratory deposition dose (TRDD) estimates and statutory limit breach (SLB) approaches. The appearance of dominating weak southern atmospheric wind flow was observed as wind speed ranged from 0 to 6.811 m/s while solar radiation periods ranged from 0.3 to 3.5 h/ day. The relative humidity of the metropolis ranged between 28 and 57%, while daily temperature was 15 to 36 °C. Highest concentration levels of PM measured were 73.4, 562.7, 7066.3 and 9907.8 $\mu g/m^3$ for $PM_{1.0}$, $PM_{2.5}$, PM_{10} and TSP, respectively. Very strong negative correlations existed between the PM concentration levels and microclimatic parameters. Spatial variation of the concentration level as modelled using Surfer® version 8 indicated that particulate concentration level increases from south to north. Concentration levels of PM for the 24-h averaging period were generally above the 24-h threshold limit value set by the regulatory agencies for all the locations.

Keywords Harmattan haze · Particulate matter · Exposure · Spatial variation · Concentration levels

J. A. Adeniran (✉) · R. O. Yusuf
Chemical Engineering, University of Ilorin, Tanke, Ilorin, Kwara State 234, Nigeria
e-mail: adeniranadetayo@yahoo.com
e-mail: adeniran.ja@unilorin.edu.ng

A. S. Aremu
Water Resources and Environmental Engineering, University of Ilorin, Ilorin, Nigeria

Y. O. Saadu
Civil Engineering, University of Ilorin, Ilorin, Nigeria

Introduction

Sub-Saharan Africa is one of the least urbanized regions in the world, but the urban population of Africa is growing very rapidly (Potts 2009). Poverty-stricken citizens of Africa, particularly in the urban population, are most negatively impacted by poor air. Sources of air pollution include those from natural and anthropogenic sources (Asubiojo 2016). It is estimated that over one billion people are exposed to open-air air pollution yearly (Zhang and Day 2015). Urban air pollution is responsible for over one million premature deaths each year in India and China (Dockery and Evans 2017). In spite of this, some mysterious and annual air pollution episodes in Africa have received less attention.

The knowledge of ambient air quality is relevant to assessing the exposure levels and providing mitigation measures. (Bose and Diette 2016; Kim et al. 2013; Shi et al. 2016). The ambient air quality depends directly on the initial concentrations of specific contaminants, the emission sources and atmospheric conditions. Air quality sampling and monitoring can be used to establish the baseline quality of regions (Seguí et al. 2016). This includes identification of specific air pollution parameters expected to have significant impacts and assessing their existing levels in ambient air within the impact zone of the study area metropolis. Among the major sources of particulate pollution are the annual Saharan dust episodes.

The prevalence of Saharan dust in the atmosphere is a common feature of the Harmattan season in most parts of sub-Saharan West Africa. Fayiga et al. (2017) posited that the largest source of ambient PM in the world is that from the Sahel-Sahara desert. The volume of Saharan dust mobilized to the world's atmosphere was estimated to range between 300 and 800 t each year (Garrison et al. 2014). The effect of this dust is most felt during the Harmattan season which normally spans between November and January. West African region is the most affected region because of its proximity to the Sahara desert. Recent studies have linked morbidity and mortality to exposure to PM emanating from Saharan dust (Adhvaryu et al. 2016; Goudie 2014; Jusot et al. 2017; Middleton 2017; Zhang et al. 2016). Inhaled dusts have a series of health effects as they affect the human respiratory and cardiovascular systems (Aubert et al. 2016; Chandrappa and Kulshrestha 2016; Okeahialam 2016). Ma et al. (2017) found a positive correlation between cases of measles and the incidence of elevated particulate (PM_{PM} and TSP) concentration levels during dust events in western China. It was observed that excess measle cases were recorded during the storm periods as compared to non-dust storm periods. Adhvaryu et al. (2016) analysed data from 12 low-income countries in West Africa over two decades and posited that dust carried by Harmattan trade wind increased infant and maternal mortality.

Aside from the health effects of Harmattan dust, it is also associated with environmental impacts such as visibility impairment, soiling of photovoltaic systems and other solar energy radiating systems (Jiang et al. 2016; Sayyah et al. 2014). Energy loss is mostly prevalent in photovoltaic generating systems as dusty modules have significantly lower operation and voltage generation (Sayyah et al. 2014). Adhvaryu et al. (2016) observed that most of the plane crash incidents in

Nigeria occurred during the Harmattan season. The study attributed it to poor visibility occasioned by the presence of high concentration of dust in the atmosphere. However due to scarcity of air pollution and health statistics in most part of Nigeria, assessment of health outcomes and statistics resulting from the annual haze episodes is limited. Monitoring of PM concentration levels is important to assist relevant stakeholders and concerned government agencies to ensure reduction in exposure and make necessary prevention strategies to curb future deleterious impact on human health. For the purpose of better understanding of the potential risk to health due to exposure to elevated levels of PM in the atmosphere, this study was conducted in Ilorin, a major urban settlement in North Central Nigeria.

Research methodology

Description of the study area

The study was carried out in Ilorin, the capital of Kwara State and one of the largest cities in Nigeria (Fig. 1). The city of Ilorin lies on longitude 8° 30′ N 4° 33′ E and latitude 8.500° N 4.550° E with daily average temperature ranges of 25 and 35 °C. The climate is equatorial with distinct wet and dry periods. With dry period (October–March) and wet period (April–September) each year. As of 2006 census, it had a population of 777,667, making it the sixth largest city in Nigeria by population. Land use patterns—residential, industrial and commercial—were considered in choosing the sampling locations in the metropolis (Table 1).

Meteorological data of the area were obtained from the University of Ilorin, Nigeria, and Lower Niger Basin Development Authority Meteorological stations.

Air sampling for PM

Heavy haze measurements were conducted on 5, 15, 18, 26 and 28 December 2016, while the light haze episode measurements were conducted on 3, 10, 11, 14, 17, 24, 30 and 31 December 2016. The visibility range considered for the light haze episodic days is 5 less than or equal to 10 km, while that of heavy haze episodic days is 0.5 less than or equal to 5 km. Particulate matter (PM) was measured with Aerocet 531S particle counter/dust monitor, an equipment from Met One Instruments. The Aerocet 531S is a full-featured, battery-operated,
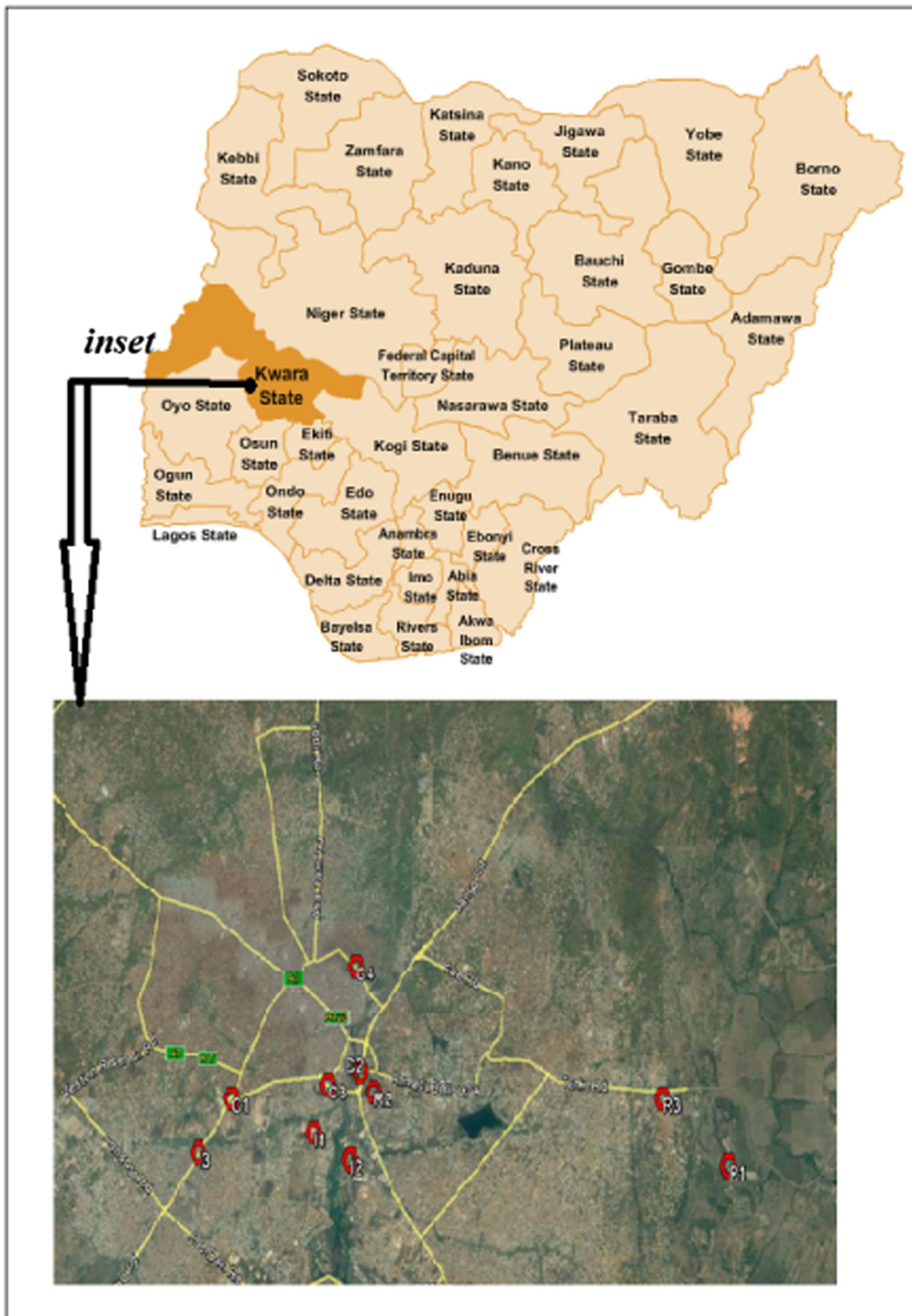
Fig. 1 Map of Nigeria showing Ilorin with the study area inset

Table 1 Sampling location and coordinates

Sampling area	Code	Category	Latitude	Longitude	Surrounding features
Unilorin Senior Staff Quarters	R1	Residential	8.469	4.643	Residential buildings
Adewole Residential Estate	R2	Residential	8.48	4.566	Residential buildings
Tanke Oke-Odo	R3	Residential	8.479	4.629	Residential buildings and shops
Dangote Flour Mill and Kam Wire Area	I1	Industrial	8.474	4.553	Smoke stacks and moving vehicles
Coca-Cola Area	I2	Industrial	8.47	4.561	Smoke stacks and moving vehicles
Sawmill	I3	Industrial	8.471	4.528	Smoke stacks and moving vehicles
Ibrahim Taiwo Road	C1	Commercial	8.479	4.535	Roadside shops, commercial buildings and heavy vehicular movement
Challenge Area	C2	Commercial	8.483	4.563	Roadside shops, commercial buildings and heavy vehicular movement
Unity Area	C3	Commercial	8.481	4.556	Major traffic intersection, commercial buildings, bakery and heavy vehicular movement
Ipata Market	C4	Commercial	8.499	4.562	Heavy vehicular movement, agricultural produce market and roadside shops

handheld mass monitor or particle counter. The unit simultaneously measures six mass concentration ranges (PM_1, $PM_{2.5}$, PM_4, PM_7, PM_{10} and TSP) or five particle count sizes (0.3, 0.5, 1.0, 5.0 and 10 μm). View sample history data in either mode. The particle counts from eight size ranges are converted to mass using a proprietary algorithm for typical density aerosols. Accommodation for special PM with different density is provided through user-programmable 'K-factors'. The standard density value is adequate for most sampling environment. To measure, it was placed between 1 and 1.5 m above the ground level (breathing zone), switched in the environment of interest and the measured concentration read directly on the screen after particle capturing. Calibration tests were carried out using Hazdust™ sampler. Gravimetric method was employed in measuring filter weights before and after sampling. The obtained PM concentrations from Hazdust™ sampler were correlated against those obtained from the Aerocet 531S dust monitor. The details of the equipment calibration have been reported in our previous study (Adeniran et al., 2017b). Corrected values were calculated using equations obtained from regressing the measured concentration of Hazdust™ sampler against that of the Aerocet 531S. Zero count tests were carried out every 1 h using the zero filter kit supplied with the Aerocet 531S dust monitors. The measurements were carried out simultaneously in all the locations.

The concentration levels measured were averaged for 1 and 8 h. The extrapolated 24-h averaging concentration was obtained using an atmospheric stability formula (Al Smadi et al., 2009) given in Eq. 1:

$$C_0 = C \times F \tag{1}$$

where

C_0 the concentration at the averaging period t_0.
C the concentration at the averaging period t_1.
F factor to convert from the averaging period t_1 to the averaging period $t_0 = (t_1 / t_0)^n$.
N 0.28, the stability dependent exponent.

Spatial variation of PM

The spatial variation in the PM measured was plotted for the light and the heavy haze episodes. The PM concentration levels obtained were used as the input data for a grid-based contour map, to study the distribution of PM sizes of 1, 2.5 and 10 and the TSP in the residential, industrial and commercial areas of Ilorin metropolis for the light and heavy haze episodes. Surfer® 8.0, a mapping software from Golden Software, LLC, USA, was used for the PM spatial distribution mapping. Kriging gridding method was adopted for the interpolation of geographical data.

Human exposure assessment

Human exposure to airborne PM at the different sampling locations was assessed using the total respiratory

deposition dose (TRDD) estimates and statutory limit breach (SLB) values of PM. The TRDD rates for PM_{10}, $PM_{2.5}$ and $PM_{1.0}$ were estimated by using the mathematical relation given by Kumar and Goel (2016) as in Eq. 2:

$$Deposited\ doses\ (in\ thoracic, tracheobronchial, alveolar\ regions)$$
$$of\ PM\ fractions = (V_T \times f) \times DF_i \times PM_i$$
$$(2)$$

where V_T is the tidal volume, f is the frequency of breathing and DF_i and PM_i are the deposition fraction and mass concentration of particle size i in micrometre. Values of V_T and f were taken as 800 cm^3 per breath and 0.35, respectively, for men during light exercise conditions (Hinds 1999; Kumar and Goel 2016). Estimates of D_{fi} for PM_{10}, $PM_{2.5}$ and PM_1 were calculated according to the equation proposed by Hinds (1999) given in Eq. 3 and inhalable fraction (IF) as given in Eq. 4.

$$DF = IF \times \left(0.058 + \frac{0.911}{1 + \exp(4.77 + In\,d_p)} + \frac{0.943}{1 + \exp(0.508 - 2.58\,In\,d_p)} \right) \quad (3)$$

$$IF = 1 - 0.5 \left(1 - \frac{1}{1 - 0.00076\,d_p^{2.8}} \right) \quad (4)$$

SLB value, expressed as the ratio of measured ambient PM concentration to the statutory limit of ambient concentration, was calculated for $PM_{2.5}$, PM_{10} and TSP using Eq. 5.

$$SLB = \frac{M_p}{S_p} \quad (5)$$

where M_p is the measured mass concentration of PM and S_P is the statutory limit of the PM. The equation was used to compute SLB value, taking into consideration the statutory limits of the US Environmental Protection Agency (USEPA 2012), Federal Ministry of Environment (FMENV) (FEPA 1991), World Bank (World Bank 1998) and that of the World Health Organization (WHO) (WHO 2006, 2010) (Table 2).

Results and discussion
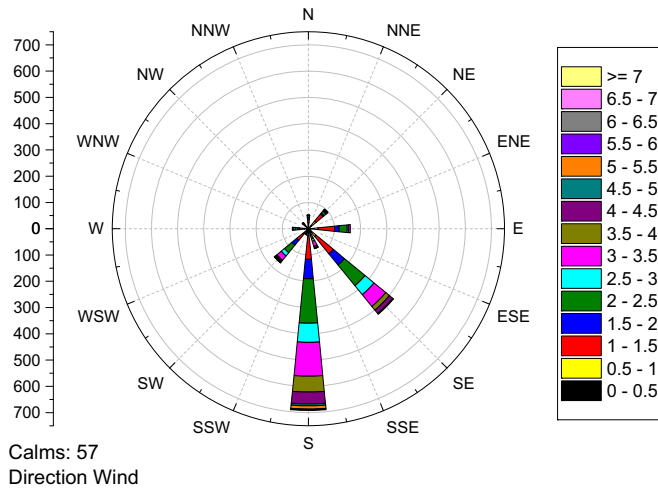
Meteorological parameters

The wind data obtained from the University of Ilorin and Lower Niger Basin Development Authority are presented in Fig. 2a, b using 1870 data sets for raw data and binned data. Wind speed ranged from 0 to 6.811 m/s with a mean and standard deviation value of 2.08 ± 1.14 m/s. As shown in Fig. 2a, the wind velocities were generally low and majorly towards southern direction. The wind speed and directions obtained in the study area are a result of the annual alternating southward and northward passages of the Intertropical Convergence Zone (ITCZ) (Sossa et al. 2017). Anuforum (2007) posited that the intertropical discontinuity (ITD) is displaced southwards during the Harmattan season. Regions around the sub-Saharan West Africa that lies between the Sahel and Gulf of Guinea are usually affected.

The appearance of dominating weak southern atmospheric wind flow inhibits the dispersion of particulate matter in the atmosphere, and this will in turn affect their

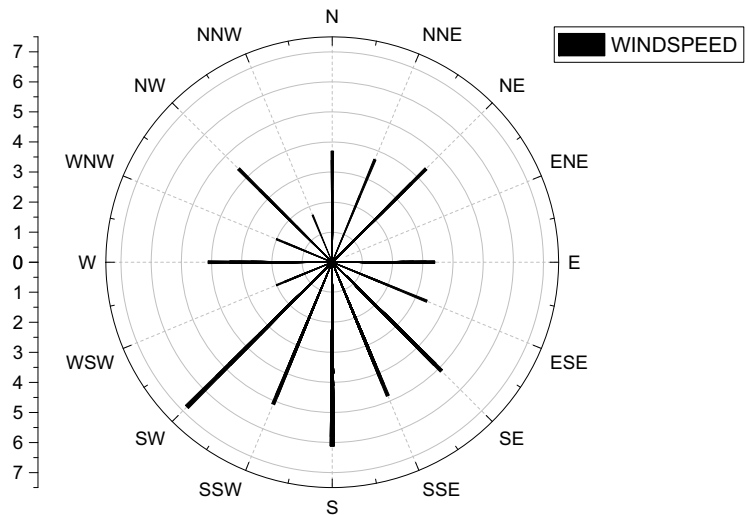Table 2 Statutory limits of particulate matter

Particulates	Concentration ($\mu g/m^3$)			
	USEPA (2012)	WHO (2006; 2010)	FEPA (1991)	WORLD BANK (1998)
$PM_{2.5}$	35 (24 h)	25 (24 h)	–	–
PM_{10}	150 (24 h)	50 (24 h)	–	–
TSP	–	–	250 (24 h)	80 (24 h)

Fig. 2 Wind rose for Ilorin metropolis during the sampling period

(a) Raw data

(b) Binned data

removal from the atmosphere (Chaloulakou et al., 2005). The descriptive statistics of other meteorological parameters such as the duration of sunshine hours per day, the relative humidity and temperature are presented in Table 3. During the heavy haze days, the high turbidity caused by the dusty air and low wind velocity had strong attenuations on the solar radiation as the period of

visible solar radiation ranged from 0.3 to 3.5 h. For the light haze days, visible solar radiation ranged from 3 to 4.1 h. The relative humidity of the metropolis ranged between 28 and 57%, while daily temperature ranged from 15 to 36 °C. The early morning and late night periods are the coldest, while the midday periods were warmer as a result of solar irradiation. No rainfall data were recorded during the study.

Concentration levels of PM

The reduction in visibility and soiling of surfaces are as a result of high concentrations of PM of various diameters in the atmosphere that were observed. The measured mass concentration of PM ($PM_{1.0}$, $PM_{2.5}$,

Table 3 Descriptive statistics of the meteorological parameters

Parameter	Min.	Max.	Mean	Standard deviation
Sunshine (h)	0.3	4.1	3.54	0.93
Relative humidity (%)	28	57	47.74	10.86
Temperature (°C)	15	36	24.5	1.85
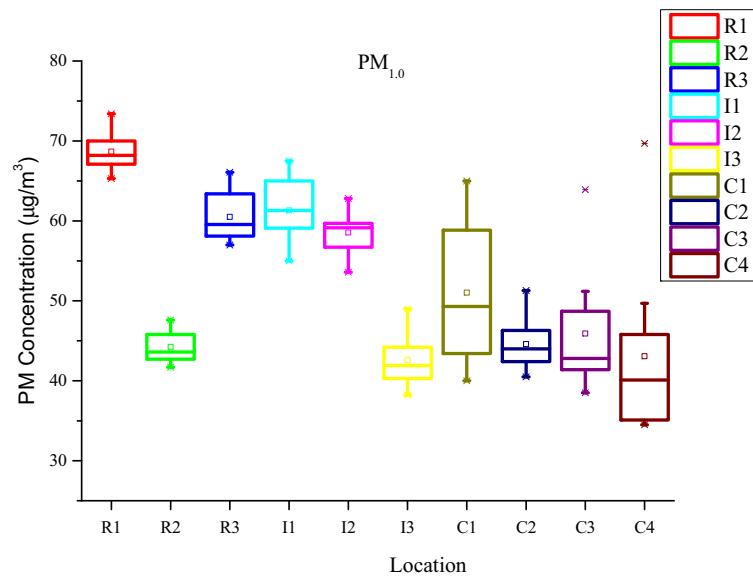
(a) Concentration levels of $PM_{1.0}$
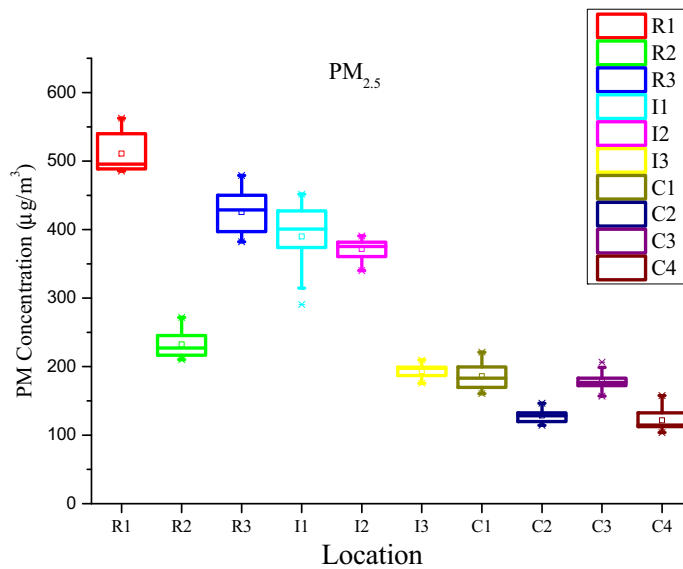
(b) Concentration levels of $PM_{2.5}$

Fig. 3 **a** Concentration levels of $PM_{1.0}$.**b** Concentration levels of $PM_{2.5}$.**c** Concentration levels of PM_{10}. **d** Concentration levels of TSP

PM_{10} and TSP) is presented in Fig. 3a–d. $PM_{1.0}$ concentration level ranged from 34.5 to 73.4 µg/ m^3; $PM_{2.5}$ ranged from 103.8 to 562.7 µg/m^3; PM_{10} ranged from 775.6 to 7066.3 µg/m^3, and the TSP concentration ranged from 1151.7 to 9907.8 µg/m^3. The mean and standard deviation values obtained for TSP in the residential areas were 6058.9 (± 364.8), 3133.5 (± 675.7) and 6624.9 (± 2012.6) µg/m^3, respectively, for R1, R2 and R3.

Similar values obtained for PM_{10}, $PM_{2.5}$ and $PM_{1.0}$ are, respectively, 4681 (± 295.4), 510.9 (± 30.0) and 68.7 (± 2.6) µg/m^3 for R1; 2090.4 (± 316.4), 232.5 (± 19.3) and 44.3 (± 1.9) µg/ m^3 for R2; and 4673 (± 1242.6), 425.7 (± 32.9) and 60.5 (± 3.1) µg/m^3 for R3. Descriptive statistics of the concentration levels were presented in the box plot for the PM sizes.

The averaged daily and 8 hourly averaged concentrations of PM are presented in Tables 4 and 5,
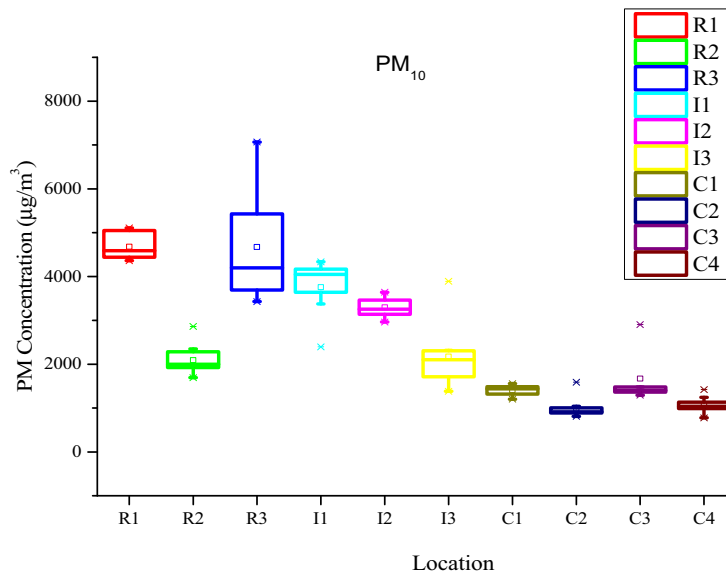
(c) Concentration levels of PM_{10}
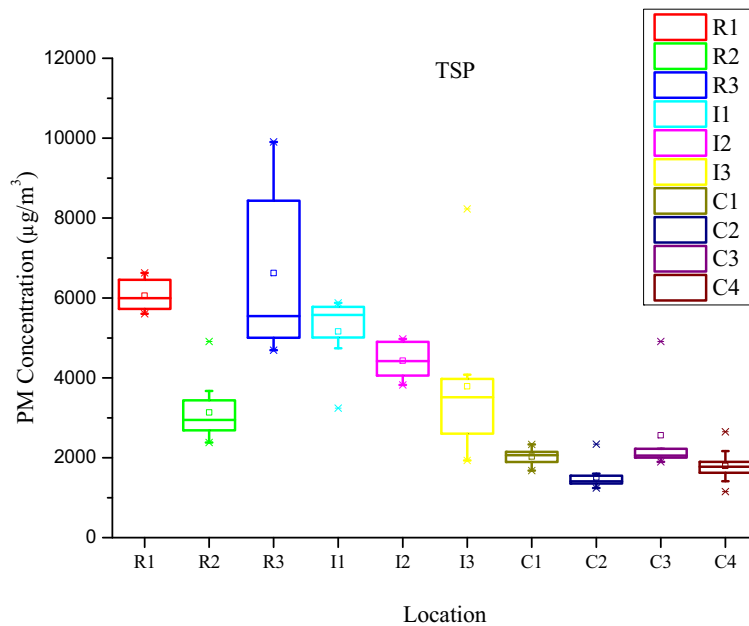
(d) Concentration levels of TSP

Fig. 3 continued.

respectively. For the daily (24 h) averaged particulate concentration, the levels obtained were 14.17–30.14, 42.63–231.09, 318.53–2902.1 and 472.98–4069 μg/m³ for $PM_{1.0}$, $PM_{2.5}$, PM_{10} and TSP, respectively. For the 8 hourly averaged concentration, the values obtained are 19.27–41.00, 57.98–314.32, 433.25–3947.24 and 643.34–5534.50 μg/m³, respectively, for $PM_{1.0}$, $PM_{2.5}$, PM_{10} and TSP. The highest PM concentrations

were obtained in R3 which is a student residential area with a lot of commercial activities. Aside from the Harmattan bound dust, other contributions to the high concentration of PM obtained include those from vehicular sources, biomass burning used in food preparation and dust resuspension from people walking. Previous study has identified heavy vehicular density in the city as a major source of airborne PM (Adeniran et al.

Table 4 Twenty-four hourly averaged concentration of particulate matter

Location	TSP ($\mu g/m^3$)				PM$_{10}$ ($\mu g/m^3$)				PM$_{2.5}$ ($\mu g/m^3$)				PM$_{1.0}$ ($\mu g/m^3$)			
	Min.	Max.	Mean	Stdev.	Min.	Max.	Mean	Stdev	Min.	Max.	Mean	Stdev.	Min.	Max.	Mean	Stdev.
R1	2301.8	2721.7	2488.3	149.8	1790.6	2097.2	1922.8	121.3	199.3	231.1	209.8	12.3	26.8	30.1	28.2	1.1
R2	977.9	2017.4	1286.9	277.5	695.2	1175.0	858.5	130.0	86.3	111.6	95.5	7.9	17.1	19.5	18.2	0.8
R3	1926.3	4069.0	2720.7	826.5	1408.5	2902.0	1919.2	510.3	157.0	196.8	174.8	13.5	23.4	27.1	24.8	1.3
I1	1332.5	2413.0	2119.8	347.5	984.6	1780.2	1542.7	249.4	119.4	185.5	160.2	19.8	22.6	27.7	25.2	1.7
I2	1571.3	2042.8	1819.9	184.4	1216.9	1495.0	1353.6	98.1	139.7	160.5	152.6	6.7	22.0	25.8	24.0	1.1
I3	794.2	3380.5	1556.6	747.2	568.4	1597.4	892.3	298.2	72.2	86.2	79.5	4.7	15.7	20.1	17.5	1.4
C1	690.1	958.0	833.4	80.8	494.4	639.5	577.2	48.2	65.9	90.8	76.4	8.6	16.4	26.7	21.0	3.7
C2	510.6	961.6	619.0	127.3	332.7	652.5	404.7	90.9	47.0	60.2	52.8	4.0	16.6	21.1	18.3	1.3
C3	780.0	2016.6	1052.8	455.8	531.0	1193.2	686.2	245.1	64.4	84.8	73.4	6.1	15.8	26.2	18.9	3.0
C4	473.0	1088.4	737.9	167.9	318.5	583.7	437.7	74.6	42.6	64.8	49.9	6.5	14.2	28.6	17.7	4.4

2017b). Total PM concentration obtained during the wet season in a previous study (Adeniran et al. 2017a) is about 11% of the TPMC obtained in the present study for the same location. The use of back-up generators in commercial buildings, roadside shops and those used in mobile telecommunications base transceiver stations also contribute to elevated airborne PM concentration levels (Adeniran et al., 2017).

The sample diurnal variation of PM concentration levels are shown in Fig. 4. The early morning and the late night periods are generally characterized by higher concentrations. This is because the wind is usually calmer in the night and there is no solar irradiation.

Lower temperature observed in the night periods also contributes to the concentration levels obtained. Cooler air is usually above making it difficult for pollutants to diffuse due to the difference in density (Janhäll et al., 2006; Sæbø et al., 2017). This phenomenon is termed temperature inversion.

The ratio of ultrafine particles (PM$_{1.0}$) to the respirable fraction (PM$_{2.5}$) to the inhalable fraction (PM$_{10}$), the respirable fraction (PM$_{2.5}$) to the inhalable fraction (PM$_{10}$) and that of the inhalable fraction to the total suspended particles was considered because of the air pollution fractions and human exposure implications.

Table 5 Eight hourly averaged concentration of particulate matter

| Location	TSP ($\mu g/m^3$)				PM$_{10}$ ($\mu g/m^3$)				PM$_{2.5}$ ($\mu g/m^3$)				PM$_{1.0}$ ($\mu g/m^3$)			
	Min.	Max.	Mean	Stdev.	Min.	Max.	Mean	Stdev.	Min.	Max.	Mean	Stdev.	Min.	Max.	Mean	Stdev.
R1	3130.8	3702.0	3384.5	203.8	2435.5	2852.6	2615.3	165.0	271.1	314.3	285.4	16.8	36.5	41.0	38.4	1.4
R2	1330.1	2744.1	1750.4	377.5	945.5	1598.2	1167.7	176.8	117.4	151.8	129.8	10.8	23.3	26.6	24.7	1.1
R3	2620.1	5534.5	3700.7	1124.2	1915.8	3947.2	2610.5	694.1	213.5	267.6	237.8	18.4	31.8	36.9	33.8	1.7
I1	1812.4	3282.1	2883.3	472.7	1339.2	2421.4	2098.3	339.3	162.4	252.3	217.8	27.0	30.7	37.7	34.3	2.4
I2	2137.2	2778.6	2475.4	250.8	1655.2	2033.4	1841.1	133.4	190.0	218.3	207.6	9.1	29.9	35.1	32.7	1.5
I3	1080.3	4598.1	2117.3	1016.3	773.2	2172.8	1213.7	405.5	98.1	117.2	108.1	6.4	21.3	27.4	23.8	1.9
C1	938.6	1303.0	1133.6	109.9	672.4	869.8	785.1	65.6	89.7	123.5	104.0	11.6	22.3	36.3	28.5	5.0
C2	694.5	1308.0	842.0	173.1	452.5	887.4	550.5	123.7	63.9	81.9	71.9	5.5	22.6	28.7	24.9	1.8
C3	1060.9	2742.9	1431.9	620.0	722.2	1623.0	933.3	333.4	87.6	115.4	99.8	8.3	21.5	35.7	25.7	4.1
C4	643.3	1480.4	1003.6	228.4	433.3	793.9	595.3	101.5	58.0	88.1	67.9	8.8	19.3	38.9	24.1	6.0
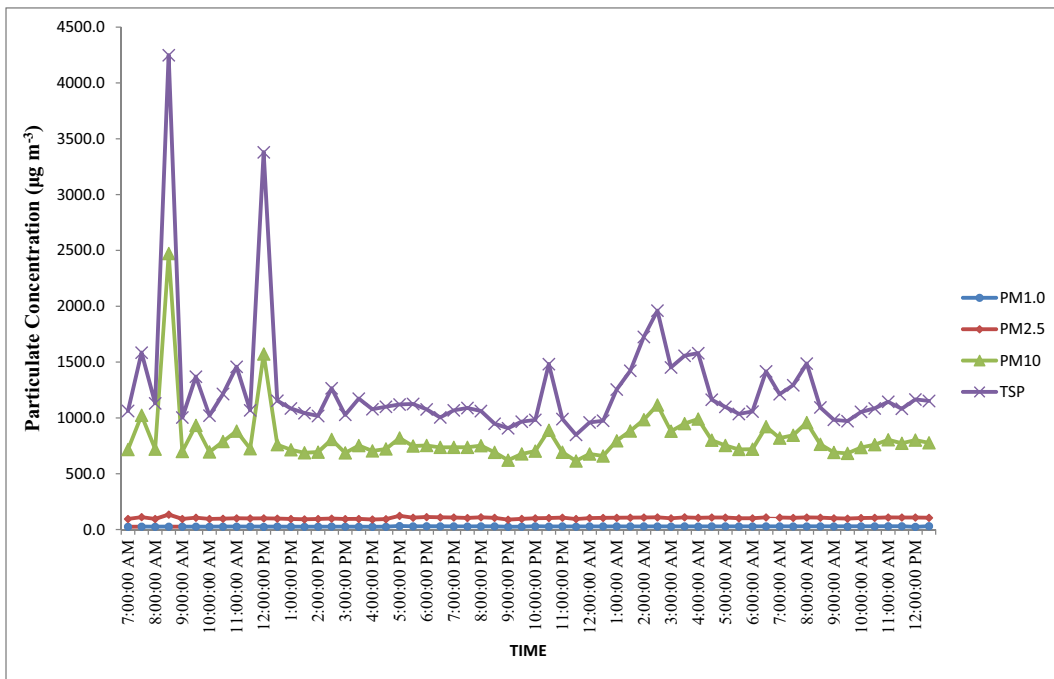
Fig. 4 Sample diurnal variation of particulate matter for hazy days

Figure 5 shows the calculated $PM_{1.0}/PM_{2.5}$, $PM_{2.5}/PM_{10}$ and PM_{10}/TSP for PM levels measured. $PM_{1.0}/PM_{2.5}$ ratio ranged from 0.13 to 0.35; $PM_{2.5}/PM_{10}$ ratio ranged from 0.09 to 0.13, while PM_{10}/TSP ratio ranged from 0.57 to 0.77. There are high percentages of coarse particles in TSP. This further corroborates the fact that concentration increases with increasing particle size due to agglomeration, accretion, coagulation and secondary formation processes. The high ratios of PM_{10}/TSP suggest that crustal materials and soil resuspension have great influence on particulate levels during dry climatic conditions.

Fig. 5 Ratios of particulate matter measured
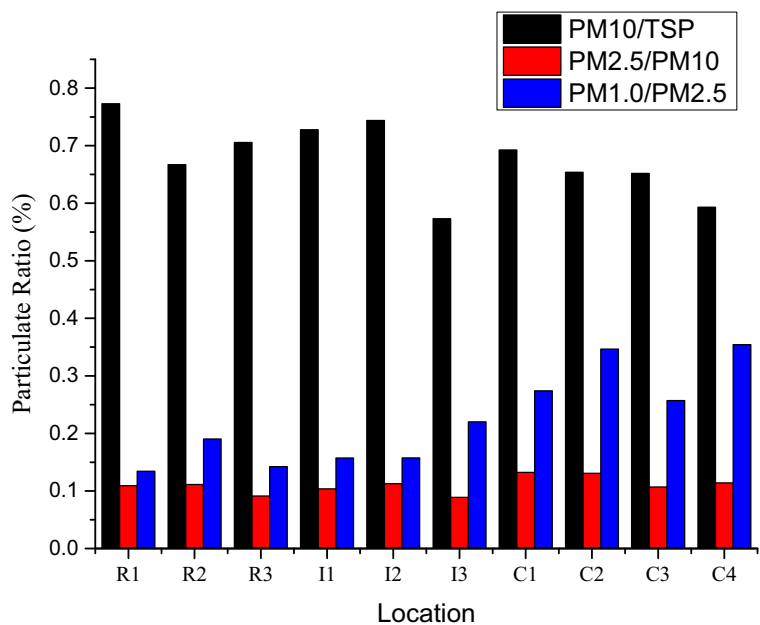
Table 6 Correlation coefficient matrix for particulates and microclimatic parameters

Factor	$PM_{1.0}$	$PM_{2.5}$	PM_{10}	TSP	WS	RH	SH	TEMP
$PM_{1.0}$	1	0.951	0.897	0.831	−0.716	−0.738	−0.783	−0.829
$PM_{2.5}$		1	0.979	0.942	−0.824	−0.846	−0.909	−0.922
PM_{10}			1	0.989	−0.884	−0.913	−0.942	−0.958
TSP				1	−0.902	−0.935	−0.940	−0.965
WS					1	0.943	0.944	0.907
RH						1	0.905	0.944
SH							1	0.911
TEMP								1

Effect of climatic parameters on haze pollution

Pearson's correlation was done using the Predictive and Analytical Software (PASW version 18). The result of Pearson's correlation to test relationships among the measured PM concentration levels and microclimatic parameters is presented in Table 6.

Strong relationships exist among all the PM sizes as the correlation coefficient obtained among them varied from 0.8 to 1.0. This indicates that lower sizes are fractions of the higher diameter particles as earlier posited. Very strong negative correlations exist between the PM concentration levels and microclimatic parameters. The obtained correlation signifies that low levels (low wind speed, low temperature, low relative humidity, less hours of sunshine) have strong impact on increased levels of airborne PM. This correlation pattern is similar to those obtained by Chaloulakou et al., 2005 who observed that strong negative correlations exist among PM and climatic parameters such as no rainfall and calm wind speed. The prevalence of stagnant or weak wind flow regimes will favour the continued suspension and accumulation of particles brought by the trade winds and those emitted locally. This will further result in the elevation of ambient PM levels. As expected, strong correlation existed between the number of sunshine hours and temperature. Wind speed and relative humidity are highly correlated with a coefficient of 0.943. The atmosphere was dry, and wind velocity was relatively calm. This condition makes airborne PM to be stable in the atmosphere.

Spatial variation of PM

The PM concentration level spatial variation contours obtained using kriging interpolation method in Surfer® v8 are presented in Figs. 6, 7, 8 and 9 for the light and heavy haze episodes. The visibility range considered for the light haze episodic days is 5 less than or equal to 10 km, while that of heavy haze episodic days is 0.5 less than or equal to 5 km. In general, several hotspots of high particulate concentrations were identified in the eight maps for $PM_{1.0}$, $PM_{2.5}$, PM_{10} and TSP.

The observed spatial variation trend observed in the metropolis further conforms with the position of Anuforom (2007) who posited that dust haze depends on latitude. The concentration increases from south to north. However, antropogenic emissions such as those from smoke stacks in the industrial region, vehicular movement, fuel combustion and other activities have influence on the particulate level on spatial scale. Some areas also fall in between mountains where dispersion of PM is further impeded by the weak flow of wind. PM especially the fine fractions ($PM_{1.0}$ and $PM_{2.5}$) tend to stay airborne for a longer period.

Exposure assessment of PM

Exposure assessment of the measured PM was done using the SLB value (comparison with the regulatory limit values) and total respiratory deposition dose.

Statutory limit breach values

In light of health concerns, several authorities have set exposure standards or guidelines for PM. Environmental Protection Agency (EPA) set a 24-h threshold limit value (24-h TLV) of 35 and 150 μg/m³ for $PM_{2.5}$ and PM_{10}, respectively, while World Health Organization (WHO) set a 24-h TLV of 25 and 50 μg/m³ for $PM_{2.5}$
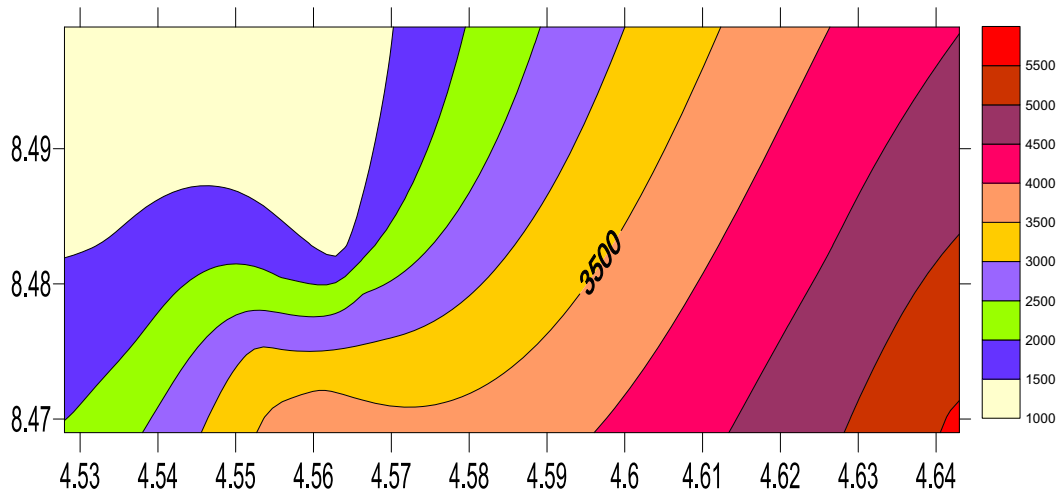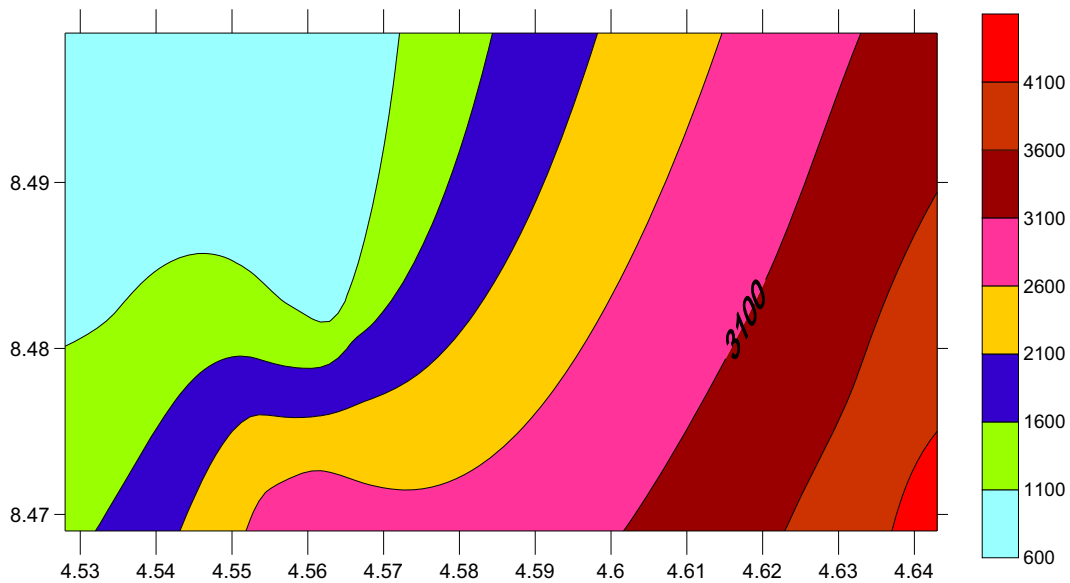
(a) Spatial variation of TSP for light haze Episode
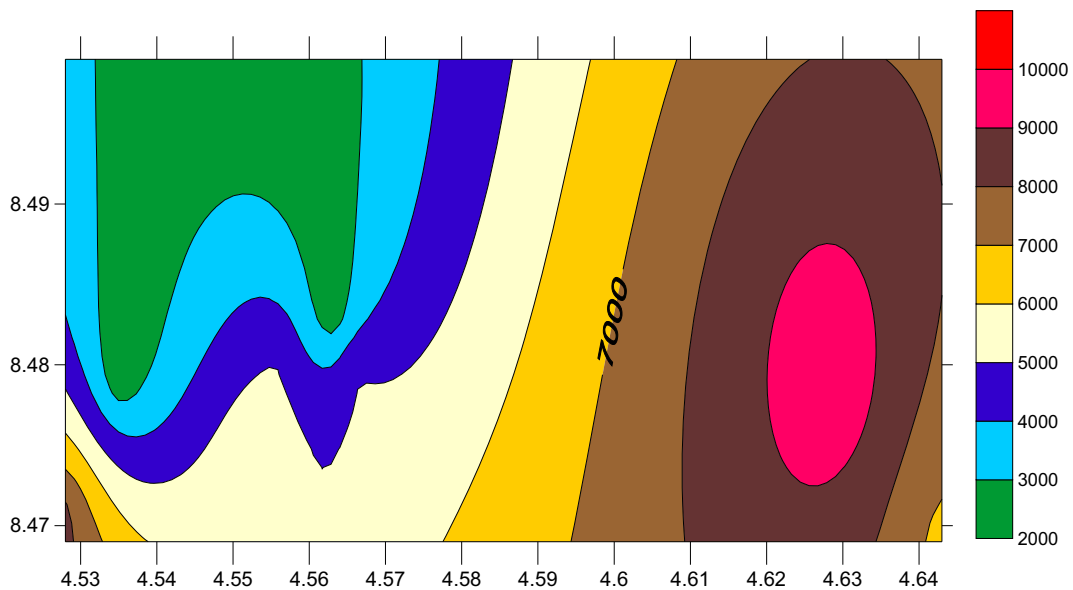
(b) Spatial variation of TSP for heavy haze episode

Fig. 6 **a** Spatial variation of TSP for light haze episode. **b** Spatial variation of TSP for heavy haze episode

and PM_{10}, respectively. For TSP, a 24-h TLV of 250 and 80 $\mu g/m^3$ was set by the Federal Ministry of Environment (now the National Environmental Standards and Regulations Enforcement Agency (NESREA)) and the World Bank, respectively. A SLB value, calculated using the threshold limits, that exceeds 1 is worrisome. SLB values of the heavy and light haze episodes are presented in Tables 7 and 8.

For the heavy haze episodes, the SLB values with reference to WHO TLV of 25 $\mu g/m^3$ for $PM_{2.5}$ ranged between 2.4 and 9.2 with an average and standard deviation of 5.1 ($\pm$ 2.4) while similar value when compared with the USEPA TLV of 35 $\mu g/m^3$ was 1.7–6.6 with an average and standard deviation of 3.7 ($\pm$ 1.7). USEPA SLB values for PM_{10} were 3.9–19.3 with an average and standard deviation of 9.4 ($\pm$ 4.9). WHO SLB values for PM_{10} were 11.7–58.0 with an average and standard deviation of 28.2 ($\pm$ 14.7). The PM concentration levels obtained also exceeded the TSP TLV of 80 $\mu g/m^3$ for World Bank in the multiples of 12.0–50.9 with an average and standard deviation of 27.1 ($\pm$ 12.9). The Nigerian FEPA TLV of 250 $\mu g/m^3$ for TSP was
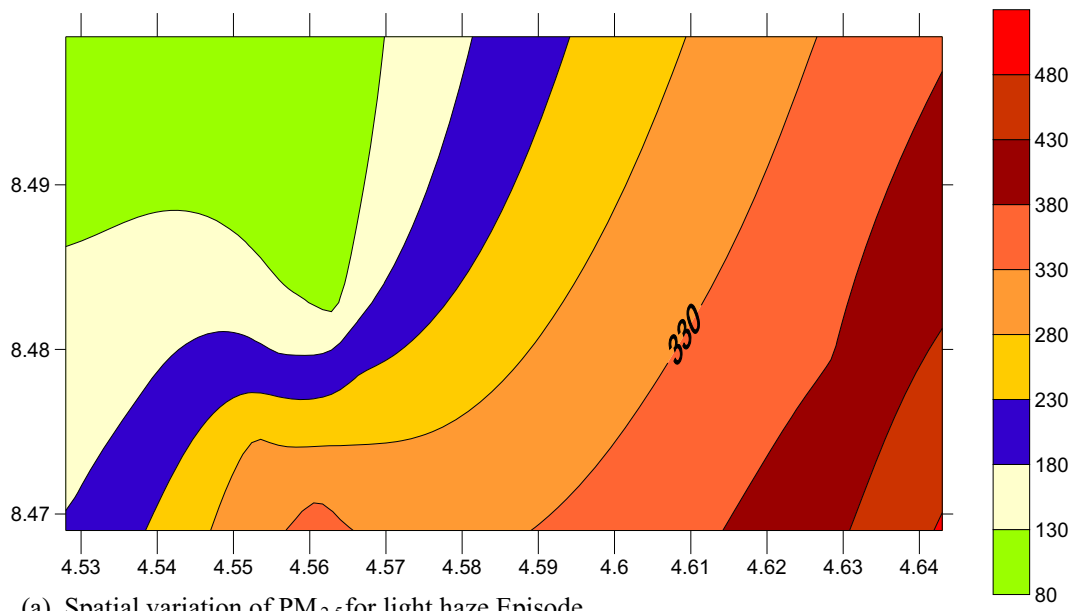
(a) Spatial variation of PM$_{10}$ for light haze Episode
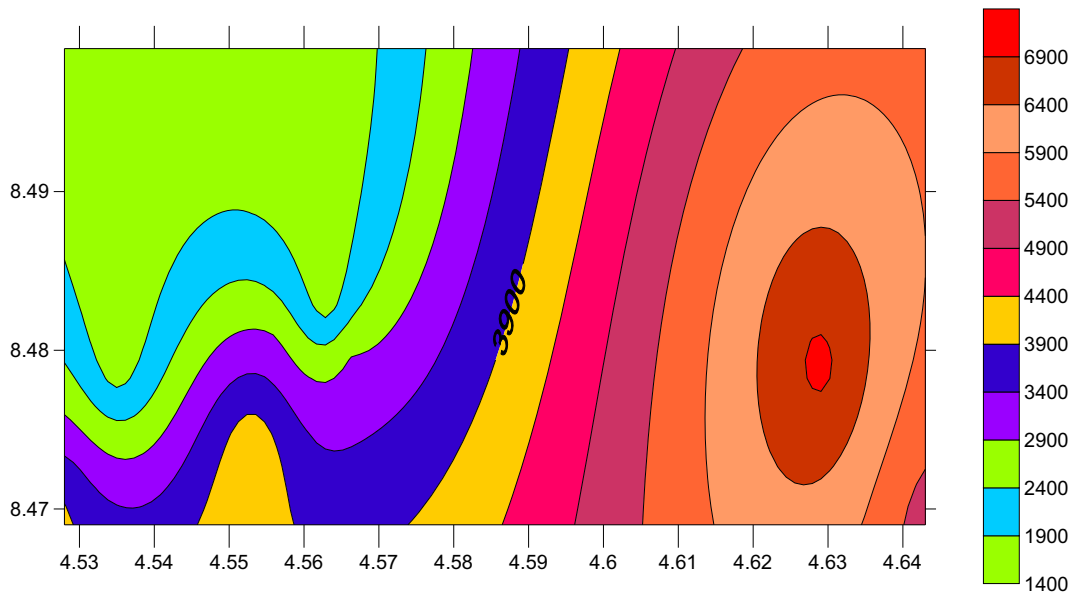
(b) Spatial variation of PM$_{10}$ for heavy haze episode

Fig. 7 **a** Spatial variation of PM$_{10}$ for light haze episode. **b** Spatial variation of PM$_{10}$ for heavy haze episode
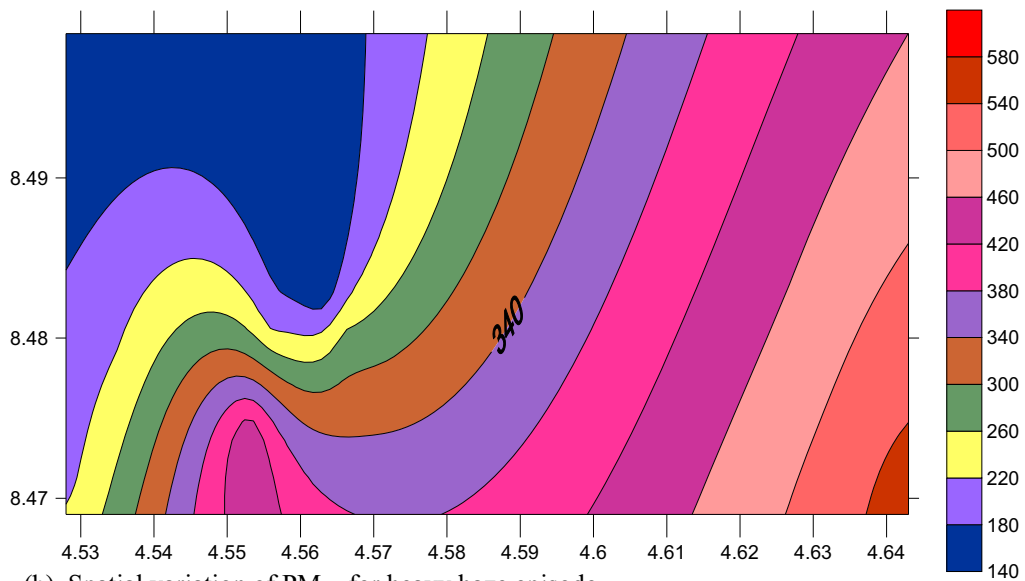
breached in the folds of 3.8–16.3 with an average and standard deviation of 8.7 ($\pm$ 4.1).

For the light haze episodes, the SLB values with reference to WHO TLV of 25 µg/m^3 for PM$_{2.5}$ ranged between 1.7 and 8.0 with an average and standard deviation of 4.0 ($\pm$ 2.1) while similar value when compared with the USEPA TLV of 35 µg/m^3 was 1.2–5.7 with an average and standard deviation of 2.8 ($\pm$ 1.5).

USEPA SLB values for PM$_{10}$ were 2.1–11.9 with an average and standard deviation of 5.6 ($\pm$ 3.3). WHO SLB values for PM$_{10}$ were 6.4–35.8 with an average and standard deviation of 16.7 ($\pm$ 10.0). The PM concentration levels obtained also exceeded the TSP TLV of 80 µg/m^3 for World Bank in the multiples of 5.90–28.8 with an average and standard deviation of 14.2 ($\pm$ 7.8). The Nigerian FEPA TLV of 250 µg/m^3 for TSP was

(a) Spatial variation of PM$_{2.5}$ for light haze Episode

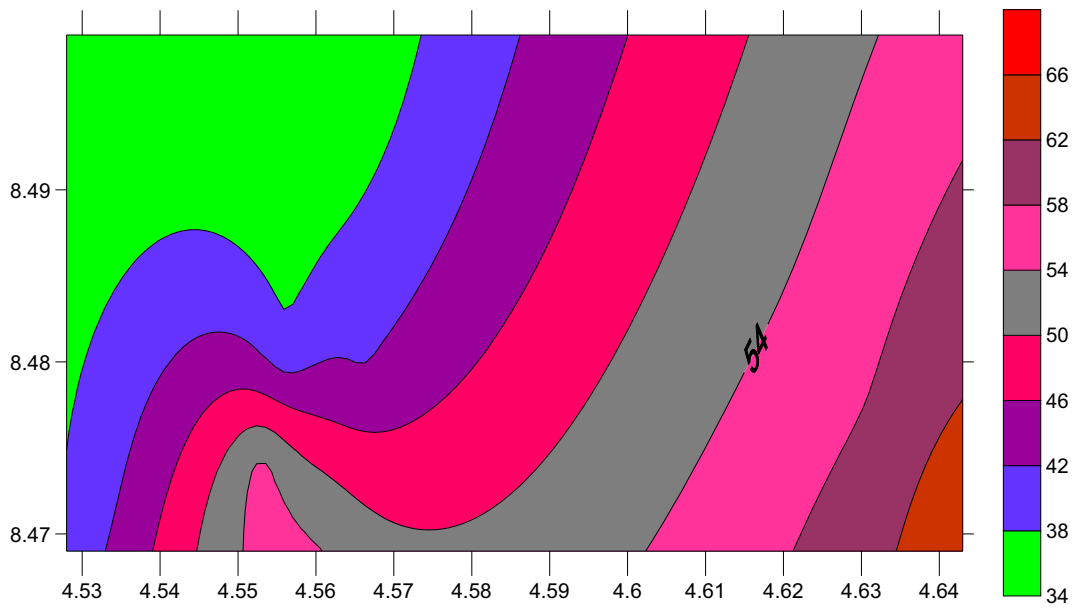(b) Spatial variation of PM$_{2.5}$ for heavy haze episode

Fig. 8 a Spatial variation of PM$_{2.5}$ for light haze episode. **b** Spatial variation of PM$_{2.5}$ for heavy haze episode

breached in the folds of 1.9–9.2 with an average and standard deviation of 4.5 (± 2.5).

Total respiratory deposition dose

The average TRDD values are presented in Fig. 10 for PM$_{10}$, PM$_{2.5}$ and PM$_{1.0}$. The TRDD for PM$_{1.0}$ were 9.68 ± 0.37, 6.29 ± 0.28, 8.53 ± 0.43, 8.78 ± 0.59, 8.26 ± 0.38, 5.97 ± 0.46, 6.95 ± 1.18, 6.29 ± 0.45, 6.48 ±

1.04 and 6.08 ± 1.52 μg/h for locations R1, R2, R3, I1, I2, I3, C1, C2, C3 and C4, respectively. The highest TRDD rate was obtained at R1, and it was about 1.63 times of the value obtained for I3. The TRDD value for PM$_{2.5}$ at R1 was 4.20 times higher than those for C4. TRDD values obtained for PM$_{2.5}$ were 149.8 ± 8.8, 69.1 ± 5.9, 124.8 ± 9.6, 116.2 ± 15.5, 109.0 ± 4.8, 57.2 ± 3.5, 53.8 ± 6.4, 37.7 ± 2.90, 52.4 ± 4.4 and 35.7 ± 4.6 μg/h for locations R1, R2, R3, I1, I2, I3, C1, C2,

(a) Spatial variation of $PM_{1.0}$ for light haze Episode
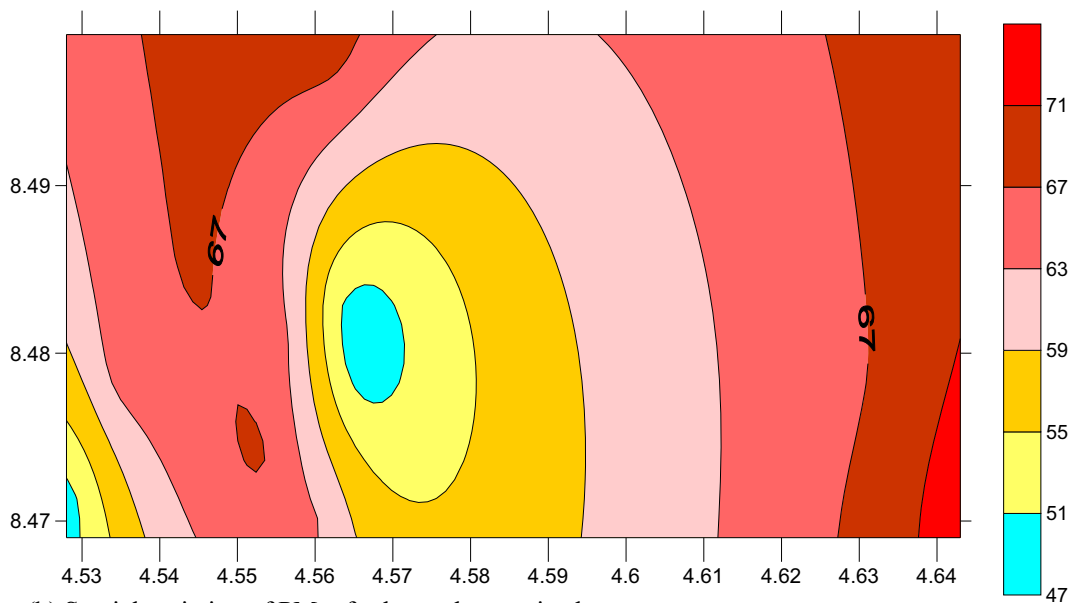
(b) Spatial variation of $PM_{1.0}$ for heavy haze episode

Fig. 9 **a** Spatial variation of $PM_{1.0}$ for light haze episode. **b** Spatial variation of $PM_{1.0}$ for heavy haze episode

C3 and C4, respectively. TRDD values estimated for PM_{10} were 1329.1 ± 83.9, 594.5 ± 98.8, 1326.6 ± 352.7, 1080.9 ± 194.9, 935.6 ± 67.8, 620.8 ± 194.7, 392.9 ± 32.9, 279.7 ± 62.8, 474.3 ± 169.4 and 302.5 ± 51.6 μg/h for locations R1, R2, R3, I1, I2, I3, C1, C2, C3 and C4, respectively. As obtained for $PM_{1.0}$ and $PM_{2.5}$, the highest TRDD value for PM_{10} was also obtained at R1; the value obtained is 4.75 times higher

than the value obtained at C2. The TRDD values obtained were on hourly basis. Multiples of the dose may be inhaled when exposed for longer hours. Road side users, market women and people who work for long hours are at greater risk. Respiratory-related ailments are often common during the hazy days. Epidemiological studies have shown that PM sizes with aerodynamic diameter less than 10 μm (PM_{10}) have adverse effect

Table 7 Average SLB values for heavy haze episodes

Location	TSP	PM$_{10}$	PM$_{2.5}$			
	FEPA	WB	USEPA	WHO	USEPA	WHO
R1	10.9	34.0	14.0	41.9	6.6	9.2
R2	8.1	25.2	7.8	23.5	3.2	4.5
R3	16.3	50.9	19.3	58.0	5.6	7.9
I1	9.7	30.2	11.9	35.6	5.3	7.4
I2	8.2	25.5	10.0	29.9	4.6	6.4
I3	13.5	42.3	10.6	31.9	2.5	3.4
C1	3.8	12.0	4.3	12.8	2.6	3.6
C2	3.8	12.0	4.3	13.0	1.7	2.4
C3	8.1	25.2	8.0	23.9	2.4	3.4
C4	4.4	13.6	3.9	11.7	1.9	2.6

on the respiratory system as they can reach the conductive airways.

Conclusion

Mass concentrations of PM (PM$_{1.0}$, PM$_{2.5}$, PM$_{10}$ and TSP) measured during the December 2016 haze episodes in 10 locations spatially distributed within Ilorin metropolis, Nigeria, reached levels considered hazardous to public health. PM$_{1.0}$ concentration level ranged from 34.5 to 73.4 μg/m^3; PM$_{2.5}$ concentration levels were between 103.8 and 562.7 μg/m^3; PM$_{10}$ ranged from 775.6 to 7066.3 μg/m^3, and the TSP concentration ranged from 1151.7 to 9907.8 μg/m^3. The appearance of dominating weak southern atmospheric wind flow observed inhibited the dispersion of PM. Pearson's correlation signifies that low levels of climatic parameters (low wind speed, low temperature, low relative humidity, less hours of sunshine) have strong impact on increased levels of airborne PM. The observed spatial variation trend observed in the metropolis indicated that PM concentration in the atmosphere increases with latitude. The concentration increases from south to north. SLB values obtained show that the averaged concentration of all the PM sizes exceeded the statutory limits set by regulatory agencies for PM$_{2.5}$, PM$_{10}$ and TSP. The highest hourly TRDD rates for PM$_{1.0}$, PM$_{2.5}$ and PM$_{10}$ were obtained at R1, while the lowest were found in I3 for PM$_{1.0}$, C4 for PM$_{2.5}$ and C2 for PM$_{10}$. In general, particulate air pollution measured reached levels considered hazardous to public health. The present study has

Table 8 Average SLB values for light haze episodes

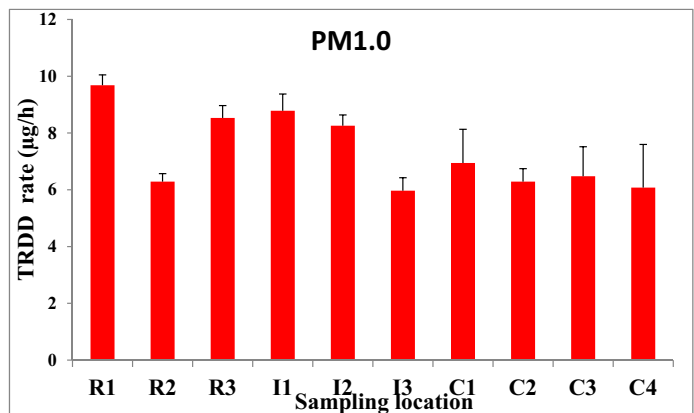| Location	TSP	PM$_{10}$	PM$_{2.5}$			
	FEPA	WB	USEPA	WHO	USEPA	WHO
R1	9.2	28.8	11.9	35.8	5.7	8.0
R2	3.9	12.2	4.6	13.9	2.5	3.5
R3	7.7	24.1	9.4	28.2	4.5	6.3
I1	5.3	16.7	6.6	19.7	3.4	4.8
I2	6.3	19.6	8.1	24.3	4.0	5.6
I3	3.2	9.9	3.8	11.4	2.1	2.9
C1	2.8	8.6	3.3	9.9	1.9	2.6
C2	2.0	6.4	2.2	6.7	1.3	1.9
C3	3.1	9.7	3.5	10.6	1.8	2.6
C4	1.9	5.9	2.1	6.4	1.2	1.7

Fig. 10 **a** TRDD levels of PM$_{10}$.
b TRDD levels of PM$_{2.5}$. **c** TRDD
levels of PM$_{1.0}$
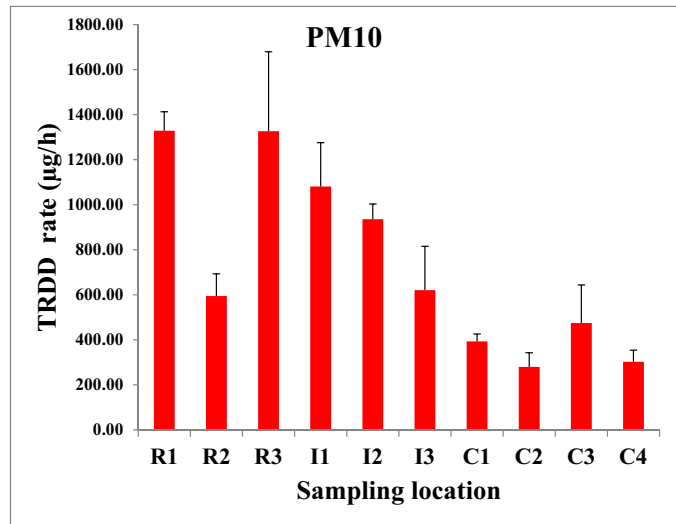
(a) TRDD levels of PM $_{10}$
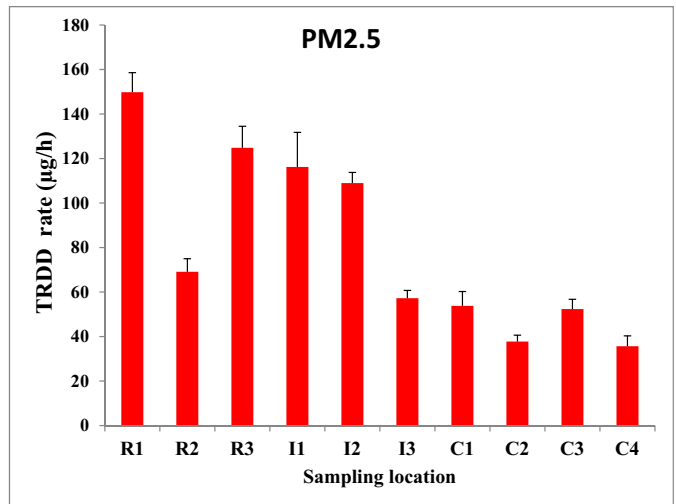
(b) TRDD levels of PM$_{2.5}$

(c) TRDD levels of PM $_{1.0}$

served as an indicator to the likely adverse consequences of elevated dose of PM during annual haze events. Public and government attention should be drawn to the inherent dangers in repeated and localized exposures. Dissemination of real-time air quality information should be made available to the public as this will contribute to increase in transparency and environmental awareness.

References

Adeniran, J., Yusuf, R., & Olajire, A. (2017a). Exposure to coarse and fine particulate matter at and around major intra-urban traffic intersections of Ilorin metropolis, Nigeria. *Atmospheric Environment, 166*, 383–392. https://doi.org/10.1016/j.atmosenv.2017.07.041.

Adeniran, J. A., Yusuf, R. O., Amole, M. O., Jimoda, L. A., & Sonibare, J. A. (2017). Air quality impact of diesel back-up generators (BUGs) in Nigeria's mobile telecommunication base transceiver stations (BTS). *Management of Environmental Quality: An International Journal, 28*(5), 723–744. https://doi.org/10.1108/MEQ-09-2015-0168.

Adeniran, J. A., Yusuf, R. O., & Olajire, A. A. (2017b). Exposure to coarse and fine particulate matter at and around major intra-urban traffic intersections of Ilorin metropolis, Nigeria. *Atmospheric Environment, 166*, 383–392. doi:https://doi.org/10.1016/j.atmosenv.2017.07.041

Adhvaryu, A., Bharadwaj, P., Fenske, J., Nyshadham, A., & Stanley, R. (2016). *Dust and death: evidence from the West African Harmattan (CSAE Working Paper WPS/2016-03).* Retrieved from Centre for the Study of African Economies: University of Oxford http://static1.1.sqspcdn.com/static/f/884336/27299906/1477070371257/ABFNSDustSept2016.pdf?token=ECCCQgzYAK%2Baw9k1HLa3L51OIVY%3D.

Al Smadi, B., Al-Zboon, K., & Shatnawi, K. (2009). Assessment of air pollutants emissions from a cement plant: a case study in Jordan. *Jordan J. Civ. Eng, 3*, 265–282.

Anuforom, A. C. (2007). Spatial distribution and temporal variability of Harmattan dust haze in sub-Sahel West Africa. *Atmospheric Environment, 41*(39), 9079–9090. https://doi.org/10.1016/j.atmosenv.2007.08.003.

Asubiojo, O. (2016). Pollution sources in the Nigerian environment and their health implications. *IFE Journal of Science, 18*(4), 973–980.

Aubert, A. E., Larina, I., Momken, I., Blanc, S., White, O., Prisk, G. K., & Linnarsson, D. (2016). Towards human exploration of space: the THESEUS review series on cardiovascular, respiratory, and renal research priorities. *npj Microgravity, 2*(16031), 1–9.

Bose, S., & Diette, G. B. (2016). Health disparities related to environmental air quality. In Gerald, L., Berry, C. (Eds.), *Health disparities in respiratory medicine* (pp. 41-58). Cham: Humana press. https://doi.org/10.1007/978-3-319-23675_3.

Chaloulakou, A., Kassomenos, P., Grivas, G., & Spyrellis, N. (2005). Particulate matter and black smoke concentration levels in central Athens, Greece. *Environment International, 31*(5), 651–659. https://doi.org/10.1016/j.envint.2004.11.001.

Chandrappa, R., & Kulshrestha, U. C. (2016). Major issues of air pollution. In sustainable air pollution management. *Environmental science and engineering* (pp. 1-48). Cham: Springer. https://doi.org/10.1007/978-3-319-215969_1.

Dockery, D. W., & Evans, J. S. (2017). Tallying the bills of mortality from air pollution. *The Lancet, 389*(10082), 1862–1864. https://doi.org/10.1016/S0140-6736(17)30884-X.

Fayiga, A. O., Ipinmoroti, M. O., & Chirenje, T. (2017). *Environmental pollution in Africa* (pp. 1–33). Development and Sustainability: Environment.

FEPA. (1991). *Guidelines to standards for environmental pollution control in Nigeria.* Lagos: Federal Environmental Protection Agency.

Garrison, V. H., Majewski, M. S., Konde, L., Wolf, R. E., Otto, R. D., & Tsuneoka, Y. (2014). Inhalable desert dust, urban emissions, and potentially biotoxic metals in urban Saharan–Sahelian air. *Science of the Total Environment, 500*, 383–394.

Goudie, A. S. (2014). Desert dust and human health disorders. *Environment International, 63*, 101–113. https://doi.org/10.1016/j.envint.2013.10.011.

Hinds, W. C. (Ed.) (1999). *Aerosol technology: properties, behaviour, and measurement of airborne particles* (2nd ed.), New York: Wiley and Sons.

Janhäll, S., Olofson, K. F. G., Andersson, P. U., Pettersson, J. B., & Hallquist, M. (2006). Evolution of the urban aerosol during winter temperature inversion episodes. *Atmospheric Environment, 40*(28), 5355–5366. https://doi.org/10.1016/j.atmosenv.2006.04.051.

Jiang, Y., Lu, L., & Lu, H. (2016). A novel model to estimate the cleaning frequency for dirty solar photovoltaic (PV) modules in desert environment. *Solar Energy, 140*, 236–240. https://doi.org/10.1016/j.solener.2016.11.016.

Jusot, J.-F., Neill, D. R., Waters, E. M., Bangert, M., Collins, M., Moreno, L. B., et al. (2017). Airborne dust and high temperatures are risk factors for invasive bacterial disease. *Journal of Allergy and Clinical Immunology, 139*(3), 977–986. e972.

Kim, H.-H., Lee, C.-S., Jeon, J.-M., Yu, S.-D., Lee, C.-W., Park, J.-H., Shin, D. C., & Lim, Y.-W. (2013). Analysis of the association between air pollution and allergic diseases exposure from nearby sources of ambient air pollution within elementary school zones in four Korean cities. *Environmental Science and Pollution Research, 20*(7), 4831–4846. https://doi.org/10.1007/s11356-012-1358-2.

Kumar, P., & Goel, A. (2016). Concentration dynamics of coarse and fine particulate matter at and around signalised traffic intersections. *Environmental Science Processes & Impacts, 18*(9), 1220–1235. https://doi.org/10.1039/C6EM00215C.

Ma, Y., Zhou, J., Yang, S., Zhao, Y., & Zheng, X. (2017). Assessment for the impact of dust events on measles incidence in western China. *Atmospheric Environment, 157*, 1–9. https://doi.org/10.1016/j.atmosenv.2017.03.010.

Middleton, N. (2017). Desert dust hazards: a global review. *Aeolian Research, 24*, 53–63. https://doi.org/10.1016/j.aeolia.2016.12.001.

Okeahialam, B. N. (2016). The cold dusty Harmattan: a season of anguish for cardiologists and patients. *Environmental health insights, 10*, 143.

Potts, D. (2009). The slowing of sub-Saharan Africa's urbanization: evidence and implications for urban livelihoods. *Environment and Urbanization, 21*(1), 253–259. https://doi.org/10.1177/0956247809103026.

Sæbø, A., Janhäll, S., Gawronski, S. W., & Hanslin, H. M. (2017). Urban forestry and pollution mitigation. *Routledge Handbook of Urban Forestry, 112*. Abingdon: Routledge.

Sayyah, A., Horenstein, M. N., & Mazumder, M. K. (2014). Energy yield loss caused by dust deposition on photovoltaic panels. *Solar Energy, 107*, 576–604. https://doi.org/10.1016/j.solener.2014.05.030.

Seguí, X., Puig, M., Quintieri, E., Wooldridge, C., & Darbra, R. M. (2016). New environmental performance baseline for inland ports: a benchmark for the European inland port sector. *Environmental Science & Policy, 58*, 29–40. https://doi.org/10.1016/j.envsci.2015.12.014.

Shi, L., Zanobetti, A., Kloog, I., Coull, B. A., Koutrakis, P., Melly, S. J., & Schwartz, J. D. (2016). Low-concentration PM2. 5 and mortality: estimating acute and chronic effects in a population-based study. *Environmental health perspectives, 124*(1), 46-52

Sossa, A., Liebmann, B., Bladé, I., Allured, D., Hendon, H. H., Peterson, P., & Hoell, A. (2017). Statistical connection between the Madden–Julian oscillation and large daily precipitation events in West Africa. *Journal of Climate, 30*(6), 1999–2010.

USEPA. (2012). *History of the National Ambient Air Quality Standards for particulate matter during the period 1971–2012*. National Ambient Air Quality: Standards.

World Health Organization. (2006). *WHO Air quality guidelines for particulate matter, ozone, nitrogendioxide and sulfur dioxide: Global update 2005-Summary of risk assessment*. Copenhagen: World HealthOrganization, 2006. Geneva: WHO.

World Health Organization. (2010). *WHO Air quality guidelines for particulate matter, ozone, nitrogendioxide and sulfur dioxide: Global update 2005-Summary of risk assessment*. Copenhagen: World HealthOrganization, 2010. Geneva: WHO.

WorldBank. (1998). Pollution Prevention and Abatement Handbook Washington DC: WORLD BANK GROUP.

Zhang, J. J., & Day, D. (2015). Urban air pollution and health in developing countries *Air Pollution and Health Effects* (pp. 355-380): Springer.

Zhang, X., Zhao, L., Tong, D. Q., Wu, G., Dan, M., & Teng, B. (2016). A systematic review of global desert dust and associated human health effects. *Atmosphere, 7*(12), 158. https://doi.org/10.3390/atmos7120158.